Developmental Biology 355 (2011) 152–162

Contents lists available at ScienceDirect

Developmental Biology

journal homepage: www.elsevier.com/developmentalbiology

Hedgehog signaling controls homeostasis of adult intestinal smooth muscle

William J. Zacharias [a,1], Blair B. Madison [b,1], Katherine E. Kretovich [a], Katherine D. Walton [a], Neil Richards [a], Aaron M. Udager [a], Xing Li [a], Deborah L. Gumucio [a,*]

[a] Department of Cell and Developmental Biology, University of Michigan, Ann Arbor MI, USA
[b] Division of Gastroenterology, Department of Medicine, University of Pennsylvania School of Medicine, Philadelphia, PA, USA

ARTICLE INFO

Article history:
Received for publication 9 February 2011
Revised 31 March 2011
Accepted 20 April 2011
Available online 28 April 2011

Keywords:
Hedgehog
Villus smooth muscle
Epithelial/mesenchymal interactions
Myocardin
Crypt proliferation
Inflammatory bowel disease
Intestinal visceral myopathy

ABSTRACT

The Hedgehog (Hh) pathway plays multiple patterning roles during development of the mammalian gastrointestinal tract, but its role in adult gut function has not been extensively examined. Here we show that chronic reduction in the combined epithelial Indian (Ihh) and Sonic (Shh) hedgehog signal leads to mislocalization of intestinal subepithelial myofibroblasts, loss of smooth muscle in villus cores and muscularis mucosa as well as crypt hyperplasia. In contrast, chronic over-expression of Ihh in the intestinal epithelium leads to progressive expansion of villus smooth muscle, but does not result in reduced epithelial proliferation. Together, these mouse models show that smooth muscle populations in the adult intestinal lamina propria are highly sensitive to the level of Hh ligand. We demonstrate further that Hh ligand drives smooth muscle differentiation in primary intestinal mesenchyme cultures and that cell-autonomous Hh signal transduction in C3H10T1/2 cells activates the smooth muscle master regulator Myocardin (Myocd) and induces smooth muscle differentiation. The rapid kinetics of *Myocd* activation by Hh ligands as well as the presence of an unusual concentration of Gli sties in this gene suggest that regulation of *Myocd* by Hh might be direct. Thus, these data indicate that Hh is a critical regulator of adult intestinal smooth muscle homeostasis and suggest an important link between Hh signaling and *Myocd* activation. Moreover, the data support the idea that lowered Hh signals promote crypt expansion and increased epithelial cell proliferation, but indicate that chronically increased Hh ligand levels do not dampen crypt proliferation as previously proposed.

Introduction

Hedgehog (Hh) signaling is a vital regulator of developmental patterning and adult homeostasis in many organ systems (reviewed in Varjosalo and Taipale, 2008). In the embryonic small intestine and colon, Hh signaling throughout life is paracrine, driven by the interaction of epithelially produced Shh and Ihh ligands with the mesenchymally expressed Patched (Ptch) receptor and signal transduction machinery (Kolterud et al., 2009). Prenatally, experimental reduction of the Hh signal in the GI tract affects the expansion of the mesenchymal compartment (Mao et al., 2010), perturbs development of the muscularis externa (Kosinski et al., 2010; Madison et al., 2005; Ramalho-Santos et al., 2000; Sukegawa et al., 2000), alters the localization of pericryptal myofibroblasts (Madison et al., 2005) and disrupts villus patterning (Kosinski et al., 2010; Madison et al., 2005; Wang et al., 2002). Through tissue cross-talk, the mesenchymal compartment, perturbed by lowered epithelial Hh levels, emits signals that feed back on the epithelium. Several investigators have observed increased epithelial Wnt signaling, enhanced progenitor cell proliferation and altered location of the proliferative compartment (Kosinski et al., 2010; Madison et al., 2005; Wang et al., 2002) upon reduction of Hh signaling.

Hh signals continue to direct epithelial/mesenchymal cross-talk in adult life. Conditional reduction of Hh levels in adult animals has been accomplished through expression of a pan-Hh inhibitor (Zacharias et al., 2010) and by epithelial-specific knockout of Ihh (van Dop et al., 2010). In both cases, mesenchymal changes included progressive myeloid inflammation, loss of differentiated smooth muscle cells (SMC) and alterations in the number and position of myofibroblasts. This mesenchymal pathology is accompanied by a robust increase in epithelial proliferation, with deep crypts but blunted villi, a histological picture that, in some but not all aspects, resembles human celiac disease. These studies indicate that Hh sits atop a signaling cascade that directs both mesenchymal and epithelial homeostasis.

In all of these studies, the two most obvious and consistent consequences of reduced Hh signals are the loss of smooth muscle differentiation in the mesenchymal compartment and the increased proliferation in the epithelial compartment. Indeed, it has been suggested that these two phenotypes could be causally connected, in that smooth muscle cells of the muscularis mucosae may comprise an important part of the epithelial stem cell niche, acting to regulate the

* Corresponding author at: Department of Cell and Developmental Biology, University of Michigan Medical School, 109 Zina Pitcher Place, 2045 BSRB, Ann Arbor, Michigan 48109-2200, USA. Fax: +1 734 647 9559.
E-mail address: dgumucio@umich.edu (D.L. Gumucio).
[1] Co-first authors contributed equally.

0012-1606/$ – see front matter © 2011 Elsevier Inc. All rights reserved.
doi:10.1016/j.ydbio.2011.04.025

number or fate of epithelial stem cells by sensing Hh levels (Kosinski et al., 2010). The idea that a negative feedback loop exists by which epithelial Hh ligands control the expression of some mesenchymal signal(s) that then feeds back to control small intestinal epithelial proliferation in a homeostatic manner had been proposed on the basis of earlier studies in the colon (van den Brink et al., 2004; van Dop et al., 2009). Though the vast majority of extant data from reduced Hh signaling models in the fetus and adult support this idea as discussed above (epithelial proliferation increases), only one previous study has examined the effects of increased Hh signal transduction on epithelial stem cell dynamics. In that study, ubiquitous activation of the Hh pathway through conditional deletion of the Ptch1 gene using a Rosa26CreERT2 driver resulted in accumulation of αSMA positive cells and crypt hypoplasia (de Santa Barbara et al., 2002). Importantly, the phenotype of this model was only studied in the colon.

The studies above have utilized conditional deletion of Ihh or of Ptch1 to study Hh signaling in the adult intestine and colon. The complete loss of Ihh or Ptch1 results in dramatic swings in Hh signal transduction that are likely seldom encountered homeostatically. To gain a better understanding of the role of Hh signaling in small intestinal homeostasis, we performed a careful analysis of two mouse models recently generated in our laboratory. Both models involve subtle alterations in Hh signaling levels. In one (Villin-Cre × Villin-Flox-Stop-Flox-Hhip, hereafter called VFHhip), Hh signaling is reduced by over-expression of a soluble version of the pan-Hh inhibitor, Hhip, while in the other (Villin-Ihh, hereafter called VIhh), Hh signaling is increased by over-expression of Ihh in the intestinal epithelium. These models modulate Hh signaling by 3–5 fold. Analyses of mice between the ages of 1 and 11 months reveal progressive pathology that includes loss of villus smooth muscle and muscularis mucosa in the context of reduced Hh signaling and significant gain of smooth muscle in the presence of increased Ihh. Thus, villus smooth muscle is exquisitely sensitive to levels of Hh ligand. Additionally, we find that Hh can drive cell-autonomous SMC differentiation in vitro. Further analysis of the pathways involved reveals that Myocardin, a master regulator of smooth muscle, is up-regulated by Hh, with kinetics similar to that seen for known Hh target genes. Additionally, as seen previously, Hh down-regulation results in increased epithelial proliferation. Surprisingly, proliferation is initially unchanged, but later increased, rather than decreased, in the context of increased Ihh.

Materials and methods

Transgenic animals

Reduced Hh signaling; the VFHhip model

These animals carry two transgenes: 12.4KVil-Cre, in which Cre recombinase is driven by the mouse villin promoter (Madison et al., 2002), and 12.4KVil-lox-LacZ-lox-HhipΔTM. The latter construct was created by the addition of the following components (from 5 to 3) into the pUC18 vector: the 12.4 kb Villin promoter ((Madison et al., 2005), available at www.addgene.org, #19358); a floxed LacZ cassette constructed from the pFlox vector (from Dr. Jamey Marth) containing a nuclear LacZ cDNA, pnlacZf (from Dr. Richard Palmiter) and bovine growth hormone polyA; HhipΔTM cDNA (Madison et al., 2005); and the SV40 late polyA/intron (from the pGL2-basic vector, Promega). Transgenic mice expressing this construct exhibit LacZ expression in intestinal epithelium (Supplemental Figs. 1A, B) and HhipΔTM cDNA is held out of frame by the floxed-LacZ cassette until excision by Cre.

For generation of transgenic mice, the vector backbone was removed and transgenic animals were created by injection into C57Bl/6 × SJL/J oocytes by the University of Michigan Transgenic Animal Core. Founders were genotyped using primers spanning the promoter/insert border (Supplemental Table 1). Five founders were utilized for the creation of transgenic lines; the two lines with the best LacZ expression without Cre were selected for further analysis. Lines were maintained on the C57Bl/6 background and generations F1 to F4 were used here. Bi-transgenic animals carrying 12.4KVil-Cre and 12.4KVil-flox-LacZ-flox-HhipΔTM are designated VFHhip.

Increased Hh signaling; the 12.4KVIhh model

The full length Ihh cDNA was amplified from newborn jejunal cDNA, and cloned into the 12.4 kb VillinΔATG vector (Addgene #19358). Transgenic animals were generated by the University of Michigan Transgenic Animal Core. Founders were genotyped using primers spanning the promoter/insert border (Supplemental Table 1). Two lines (generations F1 to F3) were analyzed. These transgenic mice, maintained on a C57Bl/6 background, are designated VIhh.

Tissue preparation, histology, and immunofluorescence

Adult whole small intestine and colonic tissue were dissected in ice-cold PBS, opened transversely, washed, fixed overnight in 4% paraformaldehyde (PFA) at 4 °C, dehydrated, infiltrated with paraffin, and sectioned at 5 μm. For frozen sectioning, intestines were fixed for 30 min. in 4% PFA at 4 °C, washed in PBS, soaked overnight in 30% sucrose in PBS, embedded in OCT, and sectioned at 6-8 μm. H&E staining was performed using standard methods. Alkaline phosphatase staining was performed using the Alkaline Phosphate Substrate Kit (Vector) and PAS/Alcian Blue staining was performed using the PAS Stain Kit (Newcomer Supply). Immunofluorescence was performed as described (Kolterud et al., 2009) using the following antibodies: mouse anti-α smooth muscle actin (Sigma, 1:500), anti-desmin (Abcam 1:500), rabbit anti-lysozyme (Zymed, 1:500), and anti-chromogranin A (Lopez-Diaz et al., 2007). All secondary antibodies used were AlexaFlour (Invitrogen, 1:500). Quantification of epithelial lineage allocation was accomplished by counting a total of 10 random 20× fields for cell number, and normalizing to the linear length of epithelium per field in microns.

RNA preparation and quantitative RT-PCR

RNA was prepared from whole adult jejunum, cultured intestinal mesenchyme, or 10T1/2 cells using Trizol (Invitrogen). cDNA was prepared using the iScript cDNA Synthesis kit (Biorad), and quantitative PCR was performed using a Biorad iCycler. Data analysis was performed using the ΔΔCt method, and fold changes were normalized to WT or vehicle treatment, as applicable. P values were calculated using Students *t*-test. Primers used in Q-RT-PCR are provided in Supplementary Table 1.

Small intestinal mesenchyme culture

Whole small intestine was harvested from E18.5 C57Bl/6 animals, cleaned of connective and pancreatic tissue, opened lengthwise, treated for 6–8 h with Cell Recovery Solution (BD Biosciences) at 4 °C to separate epithelium and mesenchyme, followed by shaking on ice as previously described (Madison et al., 2005). Separated mesenchyme was washed in sterile PBS, minced and plated in six-well plates coated with rat tail collagen (BD Biosciences) with DMEM and 10% FBS, 1 mM Hepes, and Penicillin/Streptomycin at 37 °C in 5% CO_2. Media was changed at 24 h. After 48 h, adherent mesenchyme was treated with 2.5 μg/ml recombinant mouse Shh or Ihh (R&D Systems), with or without 1 μg/ml recombinant noggin (R&D Systems) for 24 h, for a total culture of time 72 h. For RNA analysis, cells were lysed in 1 mL of Trizol (Sigma), and total RNA was prepared following the manufacturer's protocol. For immunofluorescence, mesenchyme cultured on collagen-coated coverslips was fixed for 30 min in 4% PFA at 4 °C and staining was performed utilizing antibodies described above. For quantification of IF results, 10 fields per coverslip were randomly selected, imaged and counted by three blinded observers.

Smooth muscle induction in C3H/10T1/2 cells

C3H/10T1/2 cells (clone 8) were purchased from ATCC (www.atcc.org) and maintained in DMEM with 10% FBS at 37° in 5% CO_2. Cells were passaged at 30–50% confluency to prevent differentiation. For SMC development, 6 well plates containing coverslips were seeded with 2×10^5 cells per well. Cells were cultured for 24 h in maintenance media (above), transitioned to induction media (DMEM with 0.5% FBS) for 12 h, followed by addition of TGF-β1 (10 ng/ml final), Shh (2.5 μg/mL, R&D Systems) or Ihh (2.5 μg/mL, R&D Systems), with or without noggin (1 μg/ml, R&D Systems) in induction media for 24 h. For transfection, cells were cultured to 30–50% confluency, transfected with 2 μg/well of Gli2ΔN (Roessler et al., 2005) and induced to differentiate as described above. RNA preparation, QPCR, and immunofluorescence were performed as described above.

Identification of Gli binding sites, assessment of Gli binding site enrichment, and Luciferase assays

Please see the Supplementary Methods for details of these experiments.

Statistical analysis

Statistics were calculated using the *t*-test and ANOVA functions of GraphPad Prism (www.graphpad.com). P values and test used are indicated in the corresponding figure legends.

Results

VFHhip mice: a bitransgenic model of reduced Hh signaling in postnatal intestine

To evaluate the role of Hh signaling during postnatal intestinal development and homeostasis, we created a bi-transgenic model of Hh inhibition utilizing a modified version of the previously described 12.4KVillin-HhipΔTM transgene (Madison et al., 2005). This modified transgene, 12.4KVillin-flox-LacZ-flox-HhipΔTM, uses the intestine-specific 12.4KVillin promoter (Madison et al., 2005) to drive expression of LacZ in the absence of Cre. When these mice are mated to mice carrying the intestine-specific 12.4KVillin-Cre transgene (Madison et al., 2005), excision of the LacZ cassette results in expression of HhipΔTM, a modified form of Hhip that lacks the transmembrane domain and acts as a secreted inhibitor of Hh signaling (Madison et al., 2005). We developed two independent transgenic lines of 12.4KVillin-flox-LacZ-flox-HhipΔTM with strong expression of LacZ in the small intestine, and bred each to 12.4KVilCre, which led to ablation of LacZ expression in the small intestine (Supplementary Fig. 1A, B) and caused mRNA expression of the recombined transgene VFHhip cDNA product by 1 month of age (Supplementary Fig. 1C). Expression of *Gli1* and *Ptch1*, both direct target genes of Hh signaling, were significantly reduced in response to Hhip expression at 1 month (data not shown) and 3 months of age (Supplementary Fig. 1D), confirming that this strategy leads to effective postnatal inhibition of Hh signaling.

Chronic reduction in Hh signals causes crypt hyperplasia, expansion of SMC precursors, reduced villus SM and progressive inflammation

At birth, bi-transgenic VFHhip animals appear normal and no histological changes are notable in the small intestine (data not shown). This differs from the earlier direct transgenic overexpression of Hhip, in which a robust phenotype was seen at E18.5 (Madison et al., 2005); this difference is likely due to the later activation and lower levels of Hhip in the VFHhip model compared to the previous 12.4KVil-Hhip model (data not shown). Over the next few months of post-natal life, however, crypts deepen progressively in VFHhip animals. At 3 months, crypt depth is nearly twice that of single transgenic (ST) littermates (Figs. 1A, B). Ki67 staining reveals a hyperproliferative crypt compartment; proliferative epithelial cells are detectable even above the crypt opening in VFHhip animals (Figs. 1C, D). Our previous model of Hh inhibition in the fetus also exhibited ectopic epithelial proliferation and in that model, mislocalized myofibroblasts (normally confined to crypt regions) were seen to underlie ectopic pockets of epithelial proliferation on the villi (Madison et al., 2005). Thus, we examined myofibroblast positioning in the VFHhip model. These αSMA^+ cells are confined to the crypt area in ST animals (Fig. 1E), but can be observed on villi proper in VFHhip animals (Fig. 1F).

Notably, as was observed in the fetus (Madison et al., 2005), the location of ectopic Ki67 positive epithelial cells in adults is very highly correlated with the presence of sub-epithelial myofibroblasts, suggesting a key role for myofibroblasts in controlling epithelial cell proliferation. Additionally, as in the fetus, the data suggest that Hh signals serve to restrict adult myofibroblasts to the crypt region.

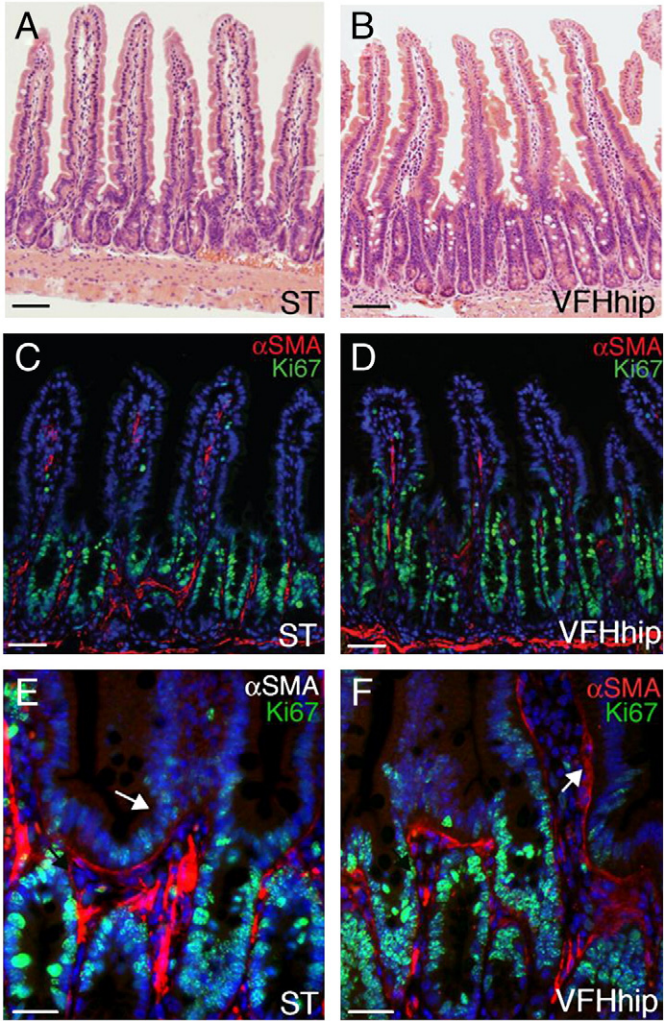

Fig. 1. Crypt hyperplasia and mislocalized myofibroblasts in VHhip mice. A, B) Histological (H&E) analysis of 3 month old single transgenic (ST, A) and VFHhip (B) animals. Note increased crypt depth. C–F) Immunostaining for αSMA (red, myofibroblast and SMC marker) and Ki67 (green, proliferation marker) in VFHhip mice and ST littermates. Proliferative epithelial cells fill the elongated crypts and are located on villus tips (D, F) in VFHhip animals. Subepithelial myofibroblasts are found farther up the crypt/villus axis in response to Hh inhibition in 1VFHhip animals, arrows, (F). Bars: A–D = 50 μm; E–F = 20 μm.

Like myofibroblasts, SMC precursors and differentiated SMC cells are direct cellular targets of Hh signaling in both fetal and adult mice (Kolterud et al., 2009; Madison et al., 2005). We therefore investigated whether postnatal inhibition of Hh signaling impacts these SMC populations. In VFHhip animals, the muscularis externa, muscularis mucosa, and villus core SMC appear normal at one month of age. However, at three months, SMC is reduced in the cores of the villi and the muscularis mucosa (Figs. 2A, B), although the muscularis externa is unaffected (not shown). In villus cores, αSMA^+;$desmin^+$ cells (differentiated SMC) are nearly absent, and αSMA^-;$desmin^+$ SMC precursor cells are expanded (Figs. 2A–D). In addition, breaks and gaps appear focally in the muscularis mucosa (arrows in Fig. 2E). These findings suggest that Hh signals are required for maintenance of villus and muscularis mucosa SMC populations during intestinal homeostasis.

Myeloid cells also transduce Hh signals and a previous study from our laboratory found a microarray signature consistent with changes in myeloid cell inflammatory phenotype in response to Hh administration in cultured intestinal lamina propria (Zacharias et al., 2010). Those studies suggested that Hh signals are required for tolerogenic myeloid cell function and that a reduction in Hh signaling leads to a pro-inflammatory phenotype in $Cd11b^+$ and $Cd11c^+$ myeloid populations. In the VFHhip mouse model, inflammation was indeed detected consistently in animals starting at 6 months of age and became progressively more prominent (Zacharias et al., 2010). Thus, it is possible that inflammatory cytokines also contributed to later expansion of the crypt zone in VFHhip animals.

Increased expression of Ihh drives smooth muscle differentiation

Since the phenotype of VFHhip animals indicates that decreased Hh signaling compromises SMC development, we tested whether increased Hh ligand production would promote SMC formation in vivo. We recently described VIhh transgenic founders, generated by linking the 12.4 kb Villin promoter to a full length Ihh cDNA (Kolterud et al., 2009). Here, we derived two transgenic lines carrying this transgene, and examined them over time for postnatal phenotypes. Effective transgene-mediated increases in the target genes *Ptch1* and *Gli1* are detectable in these mice by 3 months of age (Supplemental Fig. 2).

At birth, VIhh mice appear normal. However, analysis of villus histology by H&E reveals that by 3 months of age, villi are broad, with clefted surfaces, but no notable alteration in villus architecture (Figs. 3A–B). In animals between 1 month and 1 year old, staining with αSMA and desmin reveals very few αSMA^-;$desmin^+$ SMC precursors, but confirms a progressive increase in differentiated (αSMA^+;$desmin^+$) SMC that, by 11 months, focally distort the villus architecture (Figs. 3C–G). The expansion of smooth muscle noted in VIhh animals is confined to the villus smooth muscle population; no changes were noted in muscularis mucosa and muscularis externa smooth muscle populations at any timepoint examined.

Ki67 staining of VIhh intestines reveals that epithelial proliferation is not changed in the first three months of life (Figs. 3H–I) and is not obviously changed even later in life in areas where villus architecture is largely preserved (Fig. 3J). However, in older VIhh animals, in areas where villus morphology is disrupted by networks of interdigitated muscle, Ki67 staining demonstrates increased proliferation in adjacent epithlium (Fig. 3K). Ectopic myofibroblasts (αSMA^+;$desmin^-$) were not detectable in these regions, suggesting that signals for epithelial proliferation arose from a different cell type, possibly the amplified ectopic SMC themselves. Taken with previous findings that SMC precursors and differentiated SMC respond directly to Hh signals (Kolterud et al., 2009), these data indicate that Hh signaling drives SMC differentiation in the adult small intestine. Indeed, the adult SMC differentiation program appears to be quite responsive to the level of Hh ligand.

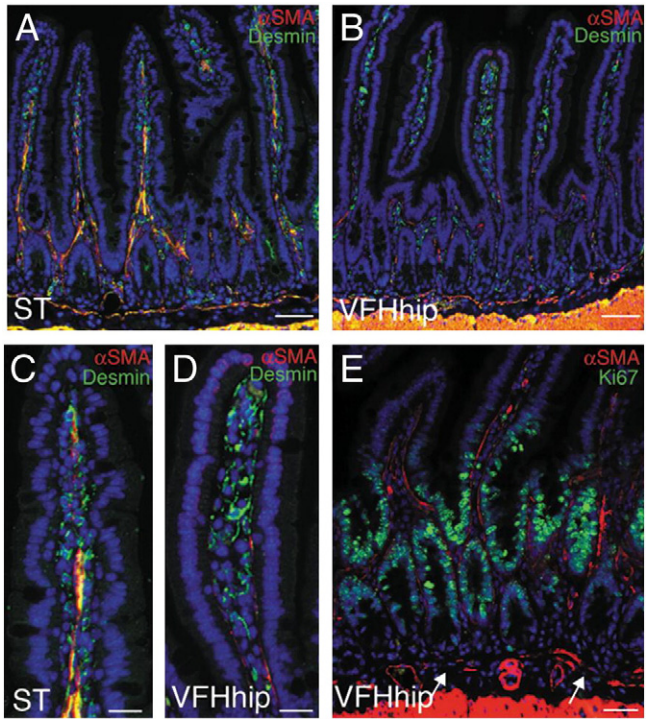

Fig. 2. Loss of differentiated SMC in VHhip mice. A–D) Immunostaining for αSMA (red) and desmin (green) reveals differentiated SMC (yellow) in the cores of villi of ST animals (A,C), but not in VFHhip animals at 3 months. SMC precursors (desmin positive only, green) are expanded in the cores of VFHhip mice (B,D). E) Focal loss of muscularis mucosa in VFHhip animals (arrows). This section is stained with αSMA and Ki67 (green, proliferation marker). Bars: A–B, E = 50 μm; C–D = 20 μm.

Hh signal modulation does not affect epithelial lineage allocation

Hh signaling in the fetal and adult intestine is paracrine, from epithelium to underlying stroma (Kolterud et al., 2009). However, epithelial characteristics may be affected indirectly and it has been proposed that altered Hh signaling can affect Paneth cell census (Varnat et al., 2006). We therefore compared VFHhip and VIhh models, assessing the differentiation of the absorptive surface and quantitating the number of Paneth cells, goblet cells and enteroendocrine cells. As shown in Fig. 4, alkaline phosphatase staining is decreased, especially at the tops of the crypts/base of the villi in VFHhip animals, suggesting that these cells are not fully differentiated, as predicted by the Ki67 results, above. In VIhh mice, alkaline phosphatase staining extends to the crypt top as in WT mice. Epithelial cell lineage allocation was not visibly altered in the context of either decreased or increased Hh signaling. Careful quantification of Paneth, goblet and enteroendocrine lineages in our models demonstrates that there is no increase or decrease in any epithelial population per micron of epithelial surface (Supplemental Fig. 3). There is an absolute increase in the number of enteroendocrine cells per villus in VIhh animals due to an increase in overall villus size, but no increase after normalization. Additionally, there are occasional Paneth cells found higher in the crypt of VFHhip animals and a small absolute increase in the Paneth cell population in the crypt, but normalization to crypt depth demonstrates no increase compared to wild type animals. Therefore, we conclude that that, in the context of 3–5 fold modulation of Hh signals, as in these models, Hh signals do not play a major role in controlling lineage allocation in the intestinal epithelium.

Hh signaling drives SMC differentiation in E18.5 intestinal mesenchyme

To confirm the role of Hh in SMC differentiation and to interrogate the pathway downstream of Hh, we examined the effect of Hh on

cultured intestinal mesenchyme from E18.5 WT and Gli1$^{+/LacZ}$ embryos. Before crypt formation, intestinal epithelium and mesenchyme can be cleanly separated; mesenchyme can be cultured for several days on a collagen matrix. Because the intestinal epithelium is the dominant source of Shh and Ihh (Kolterud et al., 2009), Hh signal transduction in isolated mesenchyme is severely reduced after 48 h in culture (Fig. 5A) as measured by lack of Xgal staining in cultures derived from Gli1$^{+/LacZ}$ animals (Bai et al., 2002). After treatment with Hh ligand for 24 h, strong LacZ expression is detectable, indicating robust Hh pathway activation (Figs. 5B, C). SMC precursor cells, myofibroblasts, and differentiated SMC are all present in vehicle treated culture after 72 h (Fig. 5D), confirming that this system is appropriate to examine the process of SMC differentiation in response to Hh pathway activation ex vivo.

We therefore treated isolated mesenchyme with vehicle, Shh, or Ihh (N = 4 wells per treatment) and quantified SM precursors, myofibroblasts, and differentiated SMC populations after 24 h. Vehicle treated mesenchyme contains a large population of αSMA^{-};desmin^{+} SM precursor cells (Fig. 5E). After treatment with Shh or Ihh, this smooth muscle precursor population is reduced by 50%, and the number of myofibroblasts and SMCs increase (Fig. 5E). These data suggest that Hh signaling promotes SMC differentiation in isolated mesenchyme, mirroring the findings seen in VIhh animals.

Myocardin, a myogenic transcription factor, is downstream of Hh signaling

The fact that SM precursors and differentiated SMC express Gli1 (Kolterud et al., 2009) suggests that the effect of Hh on these cells might be direct. To understand the molecular pathway downstream of Hh signaling, we surveyed known intracellular inducers of SMC differentiation, focusing especially on transcriptional regulators of SMC fate. Myocardin is a crucial regulator of smooth muscle differentiation (Du et al., 2003). Therefore, we examined the expression of *Myocd* in VFHhip and VIhh mice. Similar to the known Hh target genes, *Bmp4* (Fig. 6A), *Gli1* and *Ptch1* (Supplemental Fig. 1D; Supplemental Fig. 2), *Myocd* expression was increased in VIhh animals and decreased in VFHhip mice at 3 months (Fig. 6A). The decrease in *Myocd* expression seen in VFHhip animals, though not statistically significant, was reproducible. We suspect that the smaller response in these animals is due to the fact that the majority of SMC in this model is muscularis externa and this layer was not affected by down-regulation of Hh signaling in VFHhip animals.

We next confirmed that *Myocd* is activated by Shh and Ihh in isolated intestinal mesenchyme (Figs. 6B–D). Kinetic studies performed on cultured intestinal mesenchyme confirmed that *Myocd* is clearly activated within 16 h (Figs. 6C, D). Importantly, the induction of *Myocd* by Ihh or Shh occurs with similar kinetics to the induction of the known Hh targets *Gli1* and *Ptch1*, indicating that regulation could be direct (Figs. 6C, D). Another SMC expressed factor that has been shown to be involved in SMC differentiation, *Igf1*, did not respond acutely to Hh ligand addition in these cultures (Figs. 6C, D), suggesting that the response of *Myocd* is secondary to Hh induction rather than to SMC differentiation.

Hh signaling is sufficient to activate smooth muscle differentiation of C3H10T1/2 cells

Because the mesenchymal culture system is complex and contains many cells that do not respond to Hh signaling, we sought to examine the process of Hh-mediated SMC differentiation in a more homogeneous in vitro system. C3H10T1/2 is a mouse embryonic pluripotent mesenchymal cell line that expresses Ptch1 and responds to Hh

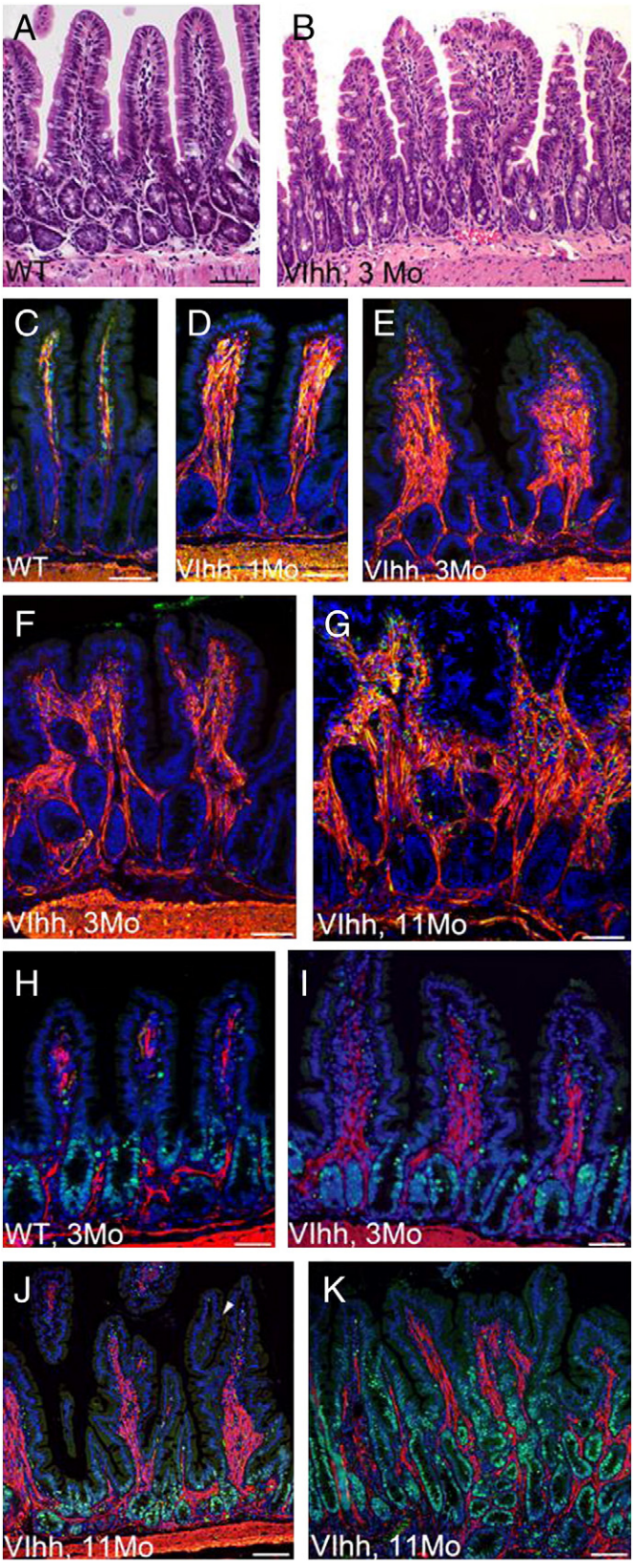

Fig. 3. Progressive expansion of villus SMC and distortion of villus and crypt architecture in VIhh mice. A,B) Histological (H&E) analysis of 3 month old WT (A) animals and VIhh (B) littermates. C–G) αSMA (red) and desmin (green) staining in WT mice (C) and VIhh mice (D–G) at ages marked on panels. Though all VIhh villi show expansion of SMC cores, areas of major distortion are focal (F,G) and increase with age. H–K) Sections are stained with αSMA (red) and Ki67 (green). At 3 months of age there is no evidence of difference in epithelial proliferation between WT mice (H) and VIhh mice (I). Later in life, the majority of the epithelium have unaltered proliferation (J), but in areas of major distortion of crypt/villus architecture, robust epithelial proliferation is seen (K). Bars = 50 μm.

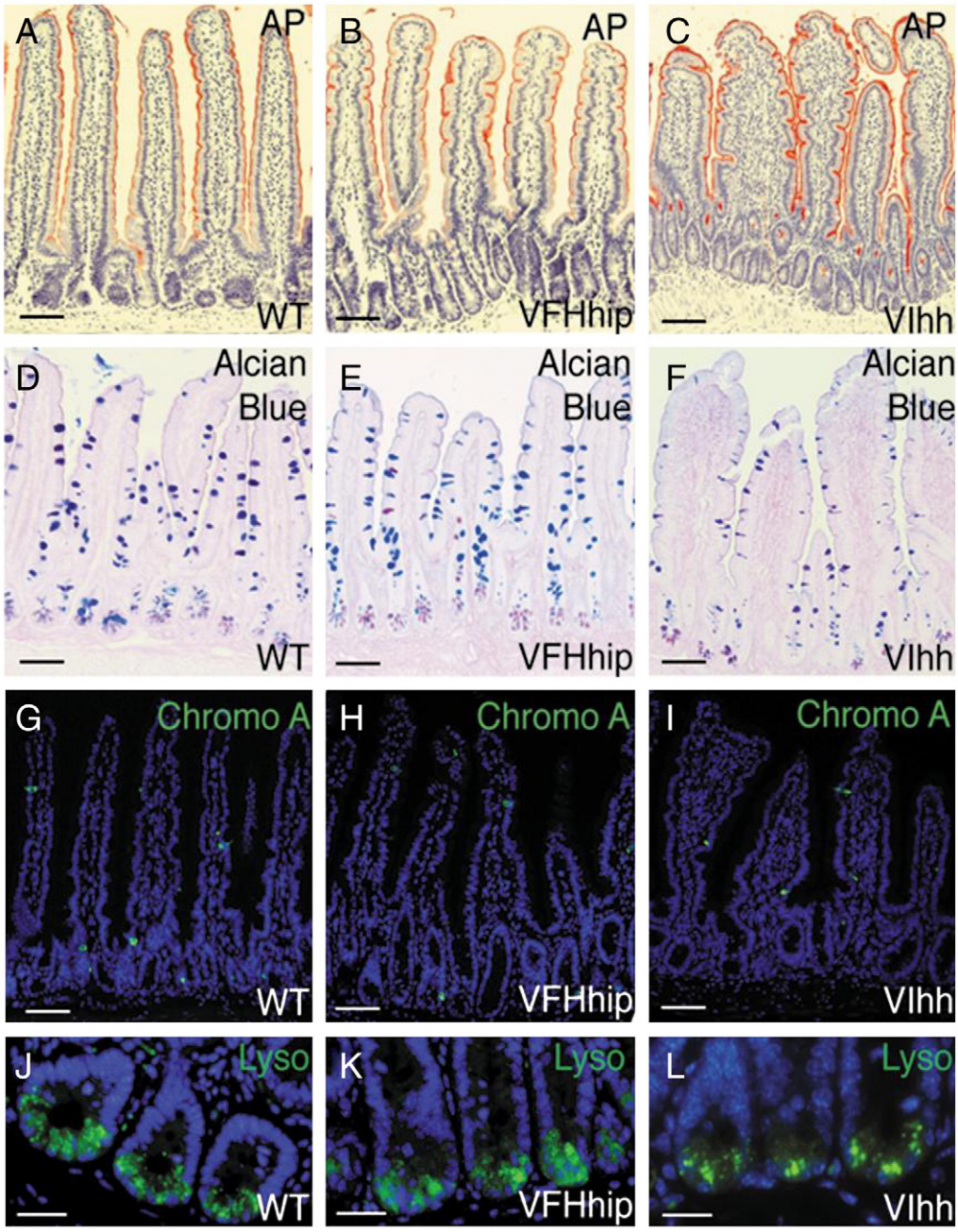

Fig. 4. Transgenic modulation of Hh signaling does not alter epithelial lineage allocation at 3 months of age. A–C) Alkaline Phosphatase (AP) staining to visualize the absorptive surface of enterocytes. The absorptive surface is reduced by expanded crypts in VFHhip animals (B) but is otherwise normal. VIhh animals (C) have similar absorptive surface to WT (A). D–F) PAS/Alcian Blue stain to visualize goblet cells. Both VFHhip (E) and VIhh (F) animals have a similar number of goblet cells compared to WT (D). G–H) Chromogranin A (Chromo A) stain for endocrine cells, with DAPI nuclear conterstain. Neither inhibition of Hh (H) nor overexpression of Hh (I) alters enteroendocrine cell number or position. J–L) Lysozyme (Lyso) staining for detection of Paneth cells, showing high magnification of crypts. No change in Paneth cell number or location is seen with Hh modulation. A–I shown at 200× magnification, J–K at 600×.

(Nakamura et al., 1997). These cells have been shown to differentiate into αSMA$^+$ SMC in response to treatment with Tgfβ1 in the presence of low serum (Lien et al., 2006). We confirmed that, in our hands, 10T1/2 cells express *Ptch1* and *Gli1* RNA as well as desmin but not αSMA protein (data not shown), suggesting that they are similar in phenotype to the smooth muscle precursor population of the mouse intestine. Thus, low passage, non-confluent 10T1/2 cells were treated with Shh, Ihh, Tgfβ1, or vehicle in low serum media and SMC differentiation was examined. As previously reported, Tgfβ1 treatment activates the SMC differentiation program as assessed by morphological change and by robust αSMA expression in the majority of cells (~70%, N = 10 wells), whereas serum withdrawal alone causes very little SMC differentiation (Figs. 7A, B). Treatment with either Shh or Ihh also causes robust SMC differentiation (N = 10 wells) (Figs. 7C, D), confirming the results seen in mesenchymal cultures.

Q-RT-PCR was used to further query the SMC differentiation program 24 h after induction with Ihh, Shh or Tgfβ1. These studies confirm that all three soluble factors induce SMC genes *αSMA*, *SM22α*, as well as *Myocd* (Fig. 7E). Notably, Shh or Ihh upregulates *Myocd* nearly two fold more robustly than Tgfβ1, though the overall degree of apparent SMC differentiation, assessed morphologically or by SMC gene expression, is similar for all three treatments.

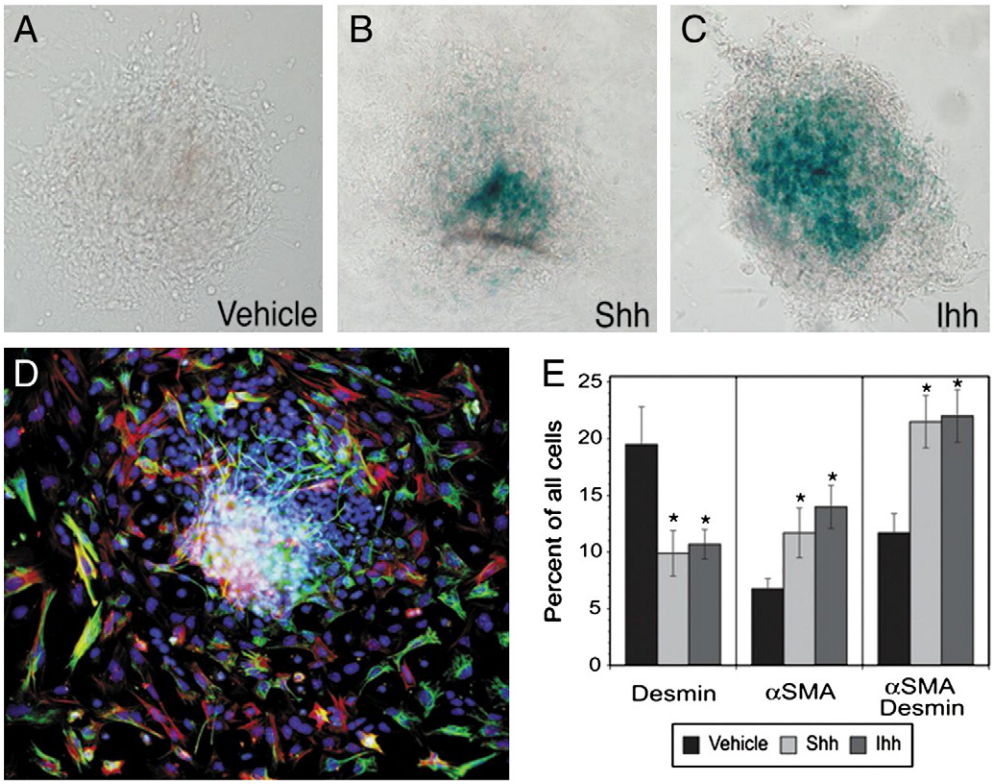

Fig. 5. Hh treatment of E18.5 mesenchyme causes Hh pathway activation, increases in myofibroblasts and SMC differentiation. A–C) Activation of Hh signaling in E18.5 $Gli1^{+/lacZ}$ mesenchyme. (A) Mesenchyme was cultured for 48 h and treated with vehicle for another 24 h. Lack of β-galactosidase activity reflects lack of active Hh signal transduction. B, C) Mesenchymal samples were held in culture for 48 h, then treated for 24 h with Shh (B) or Ihh (C). Hh signal transduction is activated. D) αSMA (red) and desmin (green) immunofluorescence demonstrates that myofibroblasts (red), SMC precursor cells (green) and differentiated SMC (yellow) are present in untreated isolated mesenchyme. E) Quantitation of myofibroblasts and SMC populations after Hh treatment in isolated WT mesenchyme. Shown are SMC precursors (Desmin), myofibroblasts (αSMA), and SMC (αSMA/Desmin) as a percentage of all cells after 24 h exposure to vehicle, Shh or Ihh. Treatment with Hh ligand decreases precursor cells and increases myofibroblasts and differentiated SMC cells. * = $p<0.05$ by Student's *t*-test compared to vehicle treatment.

A large number of Gli binding sites are present in intron 1 of mammalian Myocardin genes

The data above suggest that Hh activates SMC differentiation and that the SMC master regulator, *Myocd*, responds to Hh signals. To identify a region of the *Myocd* gene that might be responsible for this activity, we surveyed 100 kb of genomic sequence containing and surrounding the *Myocd* locus on mouse chromosome 11 for potential Gli binding sites (Supplementary Fig. 4 and Supplemental Methods). A 12 kb sequence, extending from just upstream of the transcriptional start site into intron 1, exhibited a statistically significant enrichment of Gli binding sites (Supplementary Fig. 4B). To investigate whether this region is responsible for the activation of Myocd expression downstream of Hh signaling, we cloned the Gli-enriched regions of this statistically predicted putative regulator element into Luciferase vectors, and tested whether these regions are sufficient to induce Luciferase expression in vitro (Supplementary Fig. 4). However, none of the cloned regions exhibited statistically significant Gli-dependent up-regulation of reporter activity (experimental details are presented in Supplementary Materials). Thus, we conclude that, though enriched in Gli sites, this region is not sufficient to drive the Hh-dependent expression of Myocd.

Hedgehog signals induce SMC differentiation in C3H10T1/2 cells independent of BMP and in a cell-autonomous manner

It has been suggested previously that Hh influences SMC differentiation indirectly, through the activation of *Bmp4* (Caubit et al., 2008). As we were unable to directly identify a genomic enhancer through which Hh regulates *Myocd*, we sought to investigate whether BMP signaling is required for the activation of the SMC program downstream of Hh in C3H10T1/2 cells. We therefore treated cells simultaneously with Hh and the Bmp inhibitor, noggin. Noggin treatment did not inhibit the ability of Hh to promote SMC differentiation, indicating that the mechanism of SMC differentiation downstream of Hh ligand does not require active BMP signaling (Figs. 8A–B).

Next, we asked whether Gli factors can cell autonomously drive SMC differentiation. To that end, we utilized transfection with Gli2ΔN to robustly activate the Hh pathway in specific cells in culture. We transfected C3H10T1/2 cells with Gli2ΔN, then withdrew serum to induce SMC differentiation and assessed the correlation between SMC differentiation and expression of Gli2ΔN, as detected by its Myc epitope tag (Figs. 8C–E). A total of 63% of cells transfected with Gli2ΔN expressed αSMA and took on the morphology of SMCs, compared to 8% of cells transfected with GFP alone (N = 4 independently transfected wells, Fig. 8F). In addition, non-expressing cells adjacent to Gli2ΔN-expressing cells did not develop into SMCs (Figs. 8C–E), further supporting the idea that transduction of Hh signals drives SMC differentiation in a direct, cell-autonomous manner, rather than through induction of a secondary secreted signal.

Discussion

These data demonstrate that Hh signaling is an important regulator of adult small intestinal homeostasis, with a critical role in the maintenance of smooth muscle populations in the villus core and muscularis mucosa. We show that Hh signaling is necessary and sufficient for villus smooth muscle differentiation in vivo and demonstrate in two in vitro models that Hh signaling can drive smooth muscle differentiation in a cell autonomous manner. Importantly, we show that

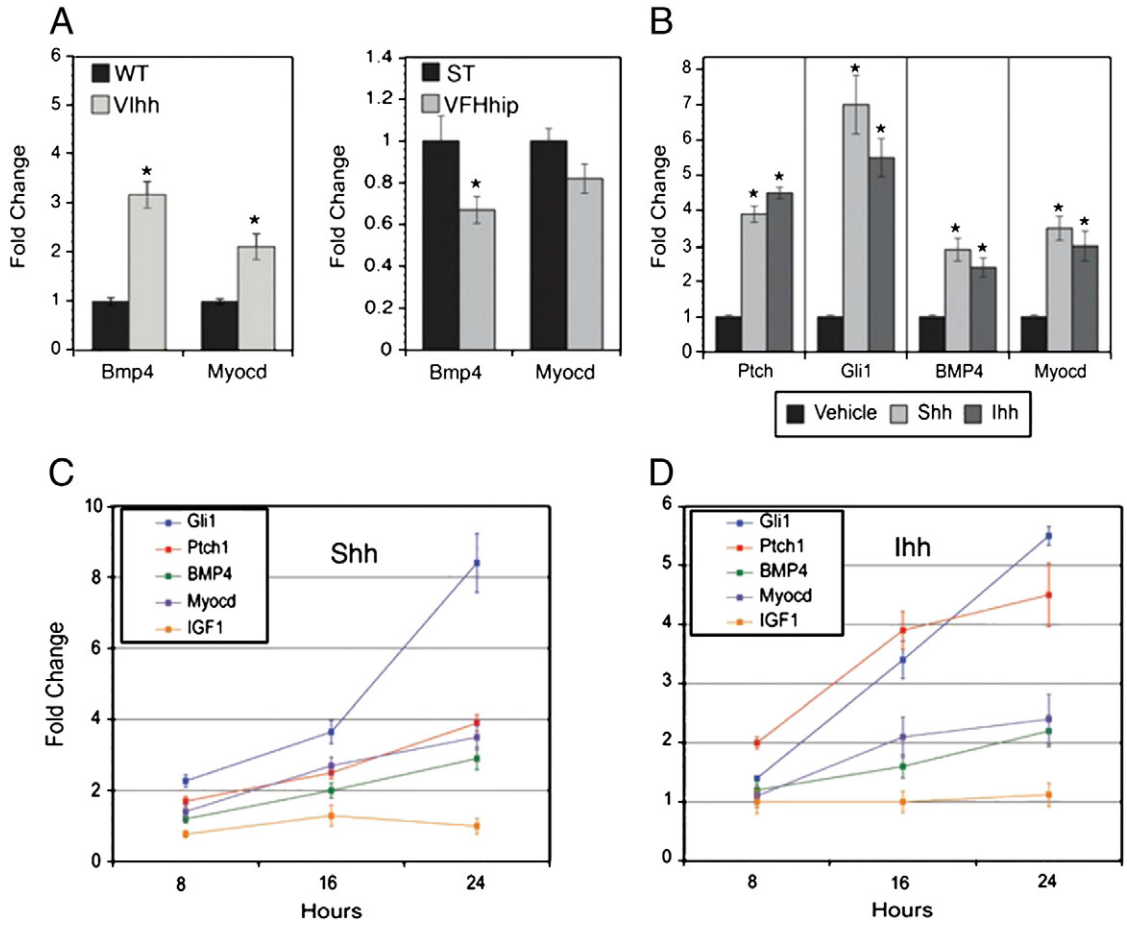

Fig. 6. Hh ligands induce *Myocd* with kinetics similar to known Hh target genes. A) Q-RT-RCR of *Bmp4* and *Myocd* expression in VIhh (left panel) and VFHhip animals (right panel). * = $p<0.05$ compared to WT or ST mice. Reduction in *Myocd* level of VFHhip animals is not significant, likely because ME is not affected in this model. B) Q-RT-PCR of *Myocd* and several Hh target genes after exposure of isolated intestinal mesenchyme to Shh or Ihh for 24 h. (Mesenchyme was held in culture for 48 h prior to treatment with Hh ligands). C, D) Time course of target gene expression after Shh (C) or Ihh (D) treatment. The kinetics of *Myocd* activation (purple line) most closely parallels the direct Hh target, *Bmp4* (green line). *Igf-1* (yellow line), also expressed by SMC, is not activated after 24 h of treatment with Hh ligand.

relatively modest alterations in Hh ligand concentration result in profound changes in villus smooth muscle mass.

In both of the mouse models described here, Hh-dependent alterations in SMC differentiation are accompanied by changes in the expression of the SMC master regulator, Myocardin. Kosinski et al. (2010) also observed that Myocd is among the prominently down-regulated genes in colon following conditional deletion of Ihh using a Villin-Cre driver. Additionally, Myocd expression was found to be reduced in the lungs of Shh null animals (Miller et al., 2004), indicating that the regulation of Myocd by Hh signaling may also occur outside the GI tract. However, these results do not clearly distinguish between modulation of Myocd as a part of the SMC differentiation program and direct transcriptional regulation of Myocd by Hh. Indeed, as shown in Fig. 7, Myocd is up-regulated (in the absence of Hh) as part of the SMC differentiation program downstream of Tgfβ, indicating that multiple signaling pathways converge on Myocd, consistent with its central role in SMC differentiation. In this context, it is noteworthy that Hh is more potent than Tgfβ as an activator of Myocd expression in the context of a similar level of SMC induction. Additionally, the kinetics of Myocd induction by Hh are suggestive of a direct response, since other known Hh target genes display similar rapid activation, while a gene associated with SMC differentiation (Igf1) does not. These findings, in association with the cell-autonomous response of Myocd to Gli2 are all congruent with the possibility that Myocd is a direct Hh target gene. In fact, we identified a region of the 5′ end of the Myocd gene that contains an unusually high concentration of Gli sites in all vertebrates examined (human, mouse, rat, dog, pig). Poisson modeling indicates that there is less than a 0.005% chance that such a cluster would occur by chance. Nevertheless, since we were unable to pinpoint the precise element(s) responsible for the transcriptional activation of Myocd by Hh, this remains an open question.

Earlier studies of the developmental patterning of ureteral muscle and embryonic intestinal muscularis externa had linked Hh signaling to the control of SMC differentiation through modulation of Bmp4 expression (Caubit et al., 2008; Sukegawa et al., 2000; Yu et al., 2002). In those settings, high levels of Hh and the ensuing high levels of Bmp are inhibitory to smooth muscle development, a characteristic that was thought to be required for the correct concentric patterning of the muscularis externa on the outside of the intestinal tube, where Hh (and Bmp) levels are low (Sukegawa et al., 2000; Yu et al., 2002). However, in our Ihh over-expressing mice, postnatal Hh signaling is increased by as much as 5 fold (as assessed by Gli1 activity, Supplemental Fig. 2). Such high Hh signals do not inhibit, but in fact robustly promote SMC development, even in areas directly adjacent to the Ihh-expressing epithelium. Moreover, even though Bmp levels are increased in VIhh intestinal mesenchyme, our in vitro studies indicate that Hh signals can, at least in some contexts, induce *Myocd* and promote SMC differentiation independently of Bmp signaling. Of course, it is also possible that Bmp and Hh signaling pathways are used in parallel. Indeed, in the chick heart, both *Myocd* and *Nkx2.5* are activated during heart development and both are important for

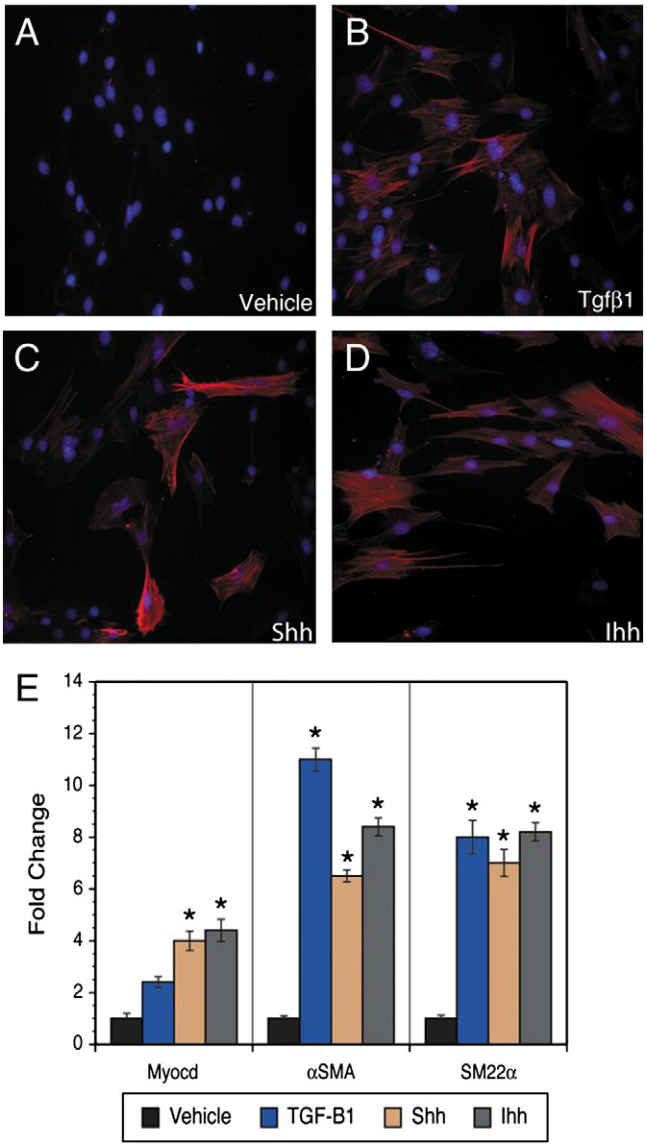

Fig. 7. Hh promotes SMC differentiation in C3H10T1/2 cells in the presence of low serum. A) 10T1/2 cells do not express *αSMA* when treated with vehicle in the presence of low serum. B) Tgfβ1 induces *αSMA* expression and morphological change in 10T1/2 cells. C, D) Shh (C) and Ihh (D) treatment drive SMC differentiation as indicated by *αSMA* expression and cell shape change in a manner similar to Tgfβ1. G) Q-RT-PCR analysis of SMC markers in 10T1/2 cells after treatment with Tgfβ1 or Hh ligand. * = $p < 0.05$ by Student's *t*-test.

cardiogenesis (Ueyama et al., 2003; Warkman et al., 2008). *Nkx2.5* expression is downstream of Bmp signaling in this system, but *Myocd* expression, though dependent upon an unknown endodermal signal, is independent of Bmp signaling (Ueyama et al., 2003; Warkman et al., 2008). It will be important to test whether the maintenance of intestinal villus smooth muscle is truly independent of Bmp signals in vivo.

Smooth muscle dysfunction is seen in several disorders and malformations of the gastrointestinal tract, including VACTERL (Kim et al., 2001; Rittler et al., 1996), irritable bowel syndrome (Choudhury et al., 2009), visceral myopathies (potentially leading to chronic pseudo-obstruction) (Antonucci et al., 2008) and mesenchymal tumors (Miettinen and Lasota, 2006), reaffirming the notion that proper control of smooth muscle populations is required for proper GI function. Our data implicate Hh and Myocardin directly in this control and show that intestinal SMC populations are very sensitive to changes in Hh levels. In this regard, it is interesting that SMC are plastic in that they can reversibly switch between a proliferative and differentiated phenotype. In mouse models of intestinal obstruction, SMC anterior to the obstruction become proliferative and later, hypertrophic (Chen et al., 2008). Potentially relevant is the fact that *Myocd* expression is reduced in the proliferative phase and activated during hypertrophy and differentiation of these cells (Chen et al., 2008). An important future goal will be to examine whether changes in Hh signal transduction are responsible for driving these adaptations. Additionally, since Hh signaling is also important in urinary, respiratory, and vascular smooth muscles, our data linking Hh to Myocardin induction may have implications for smooth muscle development and pathology in multiple organs.

In the mesenchymal compartment of the intestine, the cellular targets of Hh signals (e.g., smooth muscle precursors, differentiated smooth muscle cells, myofibroblasts) are similar in fetus and adult (Kolterud et al., 2009). As was seen in the fetus (Madison et al., 2005), we observed that reduced Hh signaling in the adult leads to mislocalization of myofibroblasts, cells that are thought to produce Wnt ligands and/or proteins that potentiate the Wnt signal, which are important in the maintenance of epithelial proliferation (Powell et al., 1999). Interestingly, ectopic crypt pockets and branched villi, characteristic aspects of the pathology associated with reduced Hh signaling in the fetus (Kosinski et al., 2010; Madison et al., 2005; Wang et al., 2002), are not seen when Hh signaling is disrupted in the adult ((van Dop et al., 2010) and this study). Indeed, crypts are expanded in VFHhip animals and areas of ectopic epithelial proliferation are seen above mislocalized myofibroblasts, but overall crypt/villus polarity is maintained. These findings indicate that villus polarity is established, in a Hh-dependent manner, in fetal life and that later reduction in Hh signaling does not disrupt polarity. However, in 11–12 month old VIhh animals, focal areas of distorted crypt architecture and branched villi are also accompanied by hyperproliferative epithelium. These areas are surrounded by extensively hypertrophied SMC (Fig. 3G), but not by myofibroblasts, suggesting that, in this setting, the signal for epithelial proliferation may emanate from the ectopic SMC and/or associated extracellular matrix. These findings suggest that two different cell types impacted by Hh signals (myofibroblasts and SMC) may be important in tightly tuning the proliferative level of the epithelial stem cell niche; either too much or too little Hh appears to promote crypt proliferation through SMC and myofibroblasts, respectively, in the adult intestine. Additionally, we and others have seen that reduced Hh signals contribute to progressive inflammation (Kosinski et al., 2010; van Dop et al., 2010; Zacharias et al., 2010). Though inflammatory infiltrates are first clearly visible in VFHhip animals at 6 months, while crypt deepening is detectable much earlier, it is not possible to rule out a role for cytokine signaling in progressive crypt expansion. These data could have important implications for colon cancer since studies in human tissues and cell lines suggest that increased Hh signaling may drive tumor growth and metastasis in late stage colon cancer (Varnat et al., 2009). Such studies provide justification for ongoing phase II clinical trials for the treatment of metastatic colorectal cancer patients with Hh antagonists (http://clinicaltrials.gov/ct2/show/NCT00636610).

It has been proposed that Hh participates in a negative feedback loop whereby differentiated epithelial cells (which express the majority of the Ihh ligand in the adult) use Hh signals to report their census and/or integrity to surrounding mesenchymal cells. When Hh levels are lowered, as in injury, the mesenchymal compartment responds by promoting epithelial proliferation via elaboration of its own soluble signals (van den Brink et al., 2004). Conversely, increases in epithelial Hh signaling are posited to instruct the mesenchyme to restrict epithelial proliferation (van den Brink et al., 2004; van Dop et al., 2009). We (and others) have confirmed that reduced Hh signal transduction results in increased proliferation, both in the fetus and in the adult (Kosinski et al., 2010; Madison et al.,

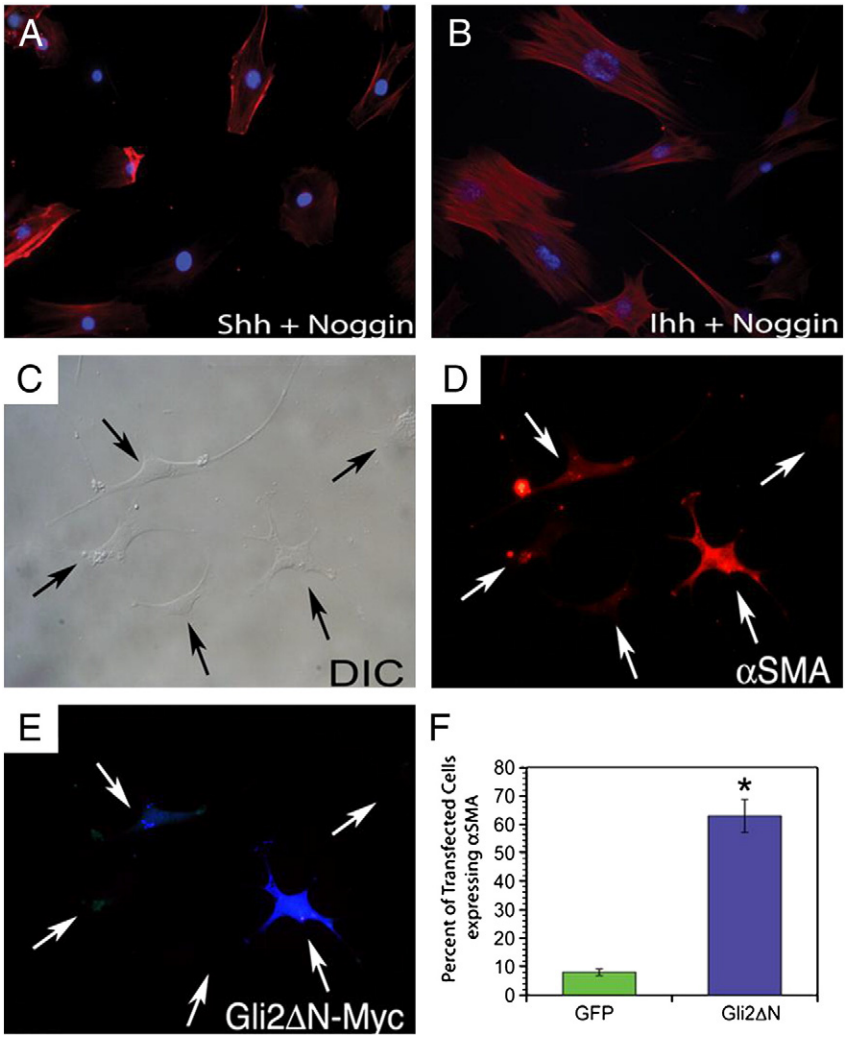

Fig. 8. Hh pathway activation is sufficient to induce cell autonomous SMC differentiation of C3H10T1/2 cells. A–B) Treatment of cells with Shh (A) or Ihh (B) in the presence of the Bmp-inhibitor, Noggin, does not alter Hh-induced *αSMA* expression in 10T1/2 cells (compare to Figs. 7C–D), indicating that Hh does not require BMP signaling to induce SMC differentiation. C–E) Gli2ΔN-transfected 10T1/2 cells exposed to differentiation media. C) DIC image; five cells are marked with arrows. D) Two cells express αSMA and take on an SMC-like morphology, whereas adjacent untransfected cells do not express αSMA. E) Staining for the Myc epitope tag confirms that these cells are positive for Gli2ΔN. F) Quantification of smooth muscle differentiation after transfection with GFP or Gli2ΔN. Ten fields from four wells in two transfection experiments were counted. * = $p<0.01$ by Student's *t*-test.

2005; van Dop et al., 2010; Wang et al., 2002). But the studies here, which are the first to examine the consequences of increased Hh signaling in the small intestine, do not support the idea that augmented Hh signaling dampens epithelial proliferation. Indeed, in older VIhh mice, chronically increased Hh ligands seem to promote, rather than inhibit, the expansion of the proliferative compartment, though this occurs in association with, and may be secondary to, severe alterations in mesenchymal patterning. The negative feedback model is also difficult to reconcile with the observation that, as villi emerge in the fetus, Shh and to some extent Ihh, are concentrated in intervillus regions where epithelial proliferation is also most prominent (Kolterud et al., 2009; Madison et al., 2005). We argue that our findings, observed after modest perturbations of Hh signaling levels (augmentation and reduction), are likely relevant to normal homeostatic regulation in the small intestine. The data presented here are most consistent with the idea that epithelial Hh signaling is being used simultaneously in (at least) two different ways in a homeostatic setting: it is necessary and sufficient for promoting SMC differentiation (a reduced Hh signal decreases and an increased Hh signal increases the amount of differentiated SMC) and it indirectly limits the extent of epithelial proliferation (too little Hh allows expansion of this compartment, but increased Hh does not further dampen proliferation).

Acknowledgments

The authors are grateful for the excellent technical assistance provided by core facilities at the University of Michigan: microscopy services by the Microscopy and Image Analysis Laboratory; tissue preparation and processing support from the Organogenesis Morphology Core; and generation of transgenic mice by the Transgenic Animal Model Core (supported by CA46592, AR20557 and DK34933). The work was supported by: grants from the NIH (R01 DK065850 to DLG), the University of Michigan Organogenesis Training Program (T32-HD007505 to WJZ) and the Hematology Training Program (T32-HL07622 to KDW).

Appendix A. Supplementary data

Supplementary data to this article can be found online at doi:10.1016/j.ydbio.2011.04.025.

References

Antonucci, A., Fronzoni, L., Cogliandro, L., Cogliandro, R.F., Caputo, C., De Giorgio, R., Pallotti, F., Barbara, G., Corinaldesi, R., Stanghellini, V., 2008. Chronic intestinal pseudo-obstruction. World J. Gastroenterol. 14, 2953–2961.

Bai, C.B., Auerbach, W., Lee, J.S., Stephen, D., Joyner, A.L., 2002. Gli2, but not Gli1, is required for initial Shh signaling and ectopic activation of the Shh pathway. Development 129, 4753–4761.

Caubit, X., Lye, C.M., Martin, E., Core, N., Long, D.A., Vola, C., Jenkins, D., Garratt, A.N., Skaer, H., Woolf, A.S., et al., 2008. Teashirt 3 is necessary for ureteral smooth muscle differentiation downstream of SHH and BMP4. Development 135, 3301–3310.

Chen, J., Chen, H., Sanders, K.M., Perrino, B.A., 2008. Regulation of SRF/CArG-dependent gene transcription during chronic partial obstruction of murine small intestine. Neurogastroenterol. Motil. 20, 829–842.

Choudhury, B.K., Shi, X.Z., Sarna, S.K., 2009. Gene plasticity in colonic circular smooth muscle cells underlies motility dysfunction in a model of postinfective IBS. Am. J. Physiol. Gastrointest. Liver Physiol. 296, G632–G642.

de Santa Barbara, P., van den Brink, G.R., Roberts, D.J., 2002. Molecular etiology of gut malformations and diseases. Am. J. Med. Genet. 115, 221–230.

Du, K.L., Ip, H.S., Li, J., Chen, M., Dandre, F., Yu, W., Lu, M.M., Owens, G.K., Parmacek, M.S., 2003. Myocardin is a critical serum response factor cofactor in the transcriptional program regulating smooth muscle cell differentiation. Mol. Cell. Biol. 23, 2425–2437.

Kim, P.C., Mo, R., Hui Cc, C., 2001. Murine models of VACTERL syndrome: role of sonic hedgehog signaling pathway. J. Pediatr. Surg. 36, 381–384.

Kolterud, A., Grosse, A.S., Zacharias, W.J., Walton, K.D., Kretovich, K.E., Madison, B.B., Waghray, M., Ferris, J.E., Hu, C., Merchant, J.L., et al., 2009. Paracrine Hedgehog signaling in stomach and intestine: new roles for hedgehog in gastrointestinal patterning. Gastroenterology 137, 618–628.

Kosinski, C., Stange, D.E., Xu, C., Chan, A.S., Ho, C., Yuen, S.T., Mifflin, R.C., Powell, D.W., Clevers, H., Leung, S.Y., Chen, X., 2010. Indian hedgehog regulates intestinal stem cell fate through epithelial-mesenchymal interactions during development. Gastroenterology 139, 893–903.

Lien, S.C., Usami, S., Chien, S., Chiu, J.J., 2006. Phosphatidylinositol 3-kinase/Akt pathway is involved in transforming growth factor-beta1-induced phenotypic modulation of 10T1/2 cells to smooth muscle cells. Cell. Signal. 18, 1270–1278.

Lopez-Diaz, L., Jain, R.N., Keely, T.M., VanDussen, K.L., Brunkan, C.S., Gumucio, D.L., Samuelson, L.C., 2007. Intestinal Neurogenin 3 directs differentiation of a bipotential secretory progenitor to endocrine cell rather than goblet cell fate. Dev. Biol. 309, 298–305. PMID:17706959.

Madison, B.B., Dunbar, L., Qiao, X.T., Braunstein, K., Braunstein, E., Gumucio, D.L., 2002. Cis elements of the villin gene control expression in restricted domains of the vertical (crypt) and horizontal (duodenum, cecum) axes of the intestine. J. Biol. Chem. 277, 33275–33283.

Madison, B.B., Braunstein, K., Kuizon, E., Portman, K., Qiao, X.T., Gumucio, D.L., 2005. Epithelial hedgehog signals pattern the intestinal crypt-villus axis. Development 132, 279–289.

Mao, J., Kim, B.M., Rajurkar, M., Shivdasani, R.A., McMahon, A.P., 2010. Hedgehog signaling controls mesenchymal growth in the developing mammalian digestive tract. Development 137, 1721–1729.

Miettinen, M., Lasota, J., 2006. Gastrointestinal stromal tumors: review on morphology, molecular pathology, prognosis, and differential diagnosis. Arch. Pathol. Lab. Med. 130, 1466–1478.

Miller, L.A., Wert, S.E., Clark, J.C., Xu, Y., Perl, A.K., Whitsett, J.A., 2004. Role of Sonic hedgehog in patterning of the tracheal-bronchial cartilage and the peripheral lung. Dev. Dyn. 231, 57–71.

Nakamura, T., Aikawa, T., Iwamoto-Enomoto, M., Iwamoto, M., Higuchi, Y., Pacifici, M., Kinto, N., Yamaguchi, A., Noji, S., Kurisu, K., et al., 1997. Induction of osteogenic differentiation by hedgehog proteins. Biochem. Biophys. Res. Commun. 237, 465–469.

Powell, D.W., Mifflin, R.C., Valentich, J.D., Crowe, S.E., Saada, J.I., West, A.B., 1999. Myofibroblasts. II. Intestinal subepithelial myofibroblasts. Am. J. Physiol. 277, C183–C201.

Ramalho-Santos, M., Melton, D.A., McMahon, A.P., 2000. Hedgehog signals regulate multiple aspects of gastrointestinal development. Development 127, 2763–2772.

Rittler, M., Paz, J.E., Castilla, E.E., 1996. VACTERL association, epidemiologic definition and delineation. Am. J. Med. Genet. 63, 529–536.

Roessler, E., Ermilov, A.N., Grange, D.K., Wang, A., Grachtchouk, M., Dlugosz, A.A., Muenke, M., 2005. A previously unidentified amino-terminal domain regulates transcriptional activity of wild-type and disease-associated human GLI2. Hum. Mol. Genet. 14, 2181–2188.

Sukegawa, A., Narita, T., Kameda, T., Saitoh, K., Nohno, T., Iba, H., Yasugi, S., Fukuda, K., 2000. The concentric structure of the developing gut is regulated by Sonic hedgehog derived from endodermal epithelium. Development 127, 1971–1980.

Ueyama, T., Kasahara, H., Ishiwata, T., Nie, Q., Izumo, S., 2003. Myocardin expression is regulated by Nkx2.5, and its function is required for cardiomyogenesis. Mol. Cell. Biol. 23, 9222–9232.

van den Brink, G.R., Bleuming, S.A., Hardwick, J.C., Schepman, B.L., Offerhaus, G.J., Keller, J.J., Nielsen, C., Gaffield, W., van Deventer, S.J., Roberts, D.J., Peppelenbosch, M.P., 2004. Indian Hedgehog is an antagonist of Wnt signaling in colonic epithelial cell differentiation. Nat. Genet. 36, 277–282.

van Dop, W.A., Uhmann, A., Wijgerde, M., Sleddens-Linkels, E., Heijmans, J., Offerhaus, G.J., van den Bergh Weerman, M.A., Boeckxstaens, G.E., Hommes, D.W., Hardwick, J.C., et al., 2009. Depletion of the colonic epithelial precursor cell compartment upon conditional activation of the hedgehog pathway. Gastroenterology 136, 2195–2203 e1-7.

van Dop, W.A., Heijmans, J., Buller, N.V., Snoek, S.A., Rosekrans, S.L., Wassenberg, E.A., van den Bergh Weerman, M.A., Lanske, B., Clarke, A.R., Winton, D.J., et al., 2010. Loss of Indian Hedgehog activates multiple aspects of a wound healing response in the mouse intestine. Gastroenterology 139, 1665–1676 1676 e1661-1610.

Varjosalo, M., Taipale, J., 2008. Hedgehog: functions and mechanisms. Genes Dev. 22, 2454–2472.

Varnat, F., Duquet, A., Malerba, M., Zbinden, M., Mas, C., Gervaz, P., Ruiz i Altaba, A., 2009. Human colon cancer epithelial cells harbour active HEDGEHOG-GLI signalling that is essential for tumour growth, recurrence, metastasis and stem cell survival and expansion. EMBO Mol. Med. 1, 338–351.

Varnat, F., Heggeler, B.B., Grisel, P., Boucard, N., Corthesy-Theulaz, I., Wahli, W., Desvergne, B., 2006. PPARbeta/delta regulates paneth cell differentiation via controlling the hedgehog signaling pathway. Gastroenterology 131, 538–553.

Wang, L.C., Nassir, F., Liu, Z.Y., Ling, L., Kuo, F., Crowell, T., Olson, D., Davidson, N.O., Burkly, L.C., 2002. Disruption of hedgehog signaling reveals a novel role in intestinal morphogenesis and intestinal-specific lipid metabolism in mice. Gastroenterology 122, 469–482.

Warkman, A.S., Yatskievych, T.A., Hardy, K.M., Krieg, P.A., Antin, P.B., 2008. Myocardin expression during avian embryonic heart development requires the endoderm but is independent of BMP signaling. Dev. Dyn. 237, 216–221.

Yu, J., Carroll, T.J., McMahon, A.P., 2002. Sonic hedgehog regulates proliferation and differentiation of mesenchymal cells in the mouse metanephric kidney. Development 129, 5301–5312.

Zacharias, W.J., Li, X., Madison, B.B., Kretovich, K., Kao, J.Y., Merchant, J.L., Gumucio, D.L., 2010. Hedgehog is an anti-inflammatory epithelial signal for the intestinal lamina propria. Gastroenterology 138, 2368–2377 2377 e2361-2364.